韓國精密工學會 '97年度 秋季學術大會論文集 pp.1089~1092

정전력 구동 및 전자력 검출형 평면 진동 각속도계
Planar Vibratory Gyroscope using Electrostatic Actuation and Electromagnetic Detection

*이상훈(서울대 대학원), 임형택(서울대 대학원), 이승기(단국대 공대), 김용권(서울대 공대)
Sang-Hun Lee(Graduate School, Seoul Nat' l Univ), Hyung-Taek Lim(Graduate School, Seoul Nat' l Univ)
Seung-Ki Lee(Dankook Univ), Yong-Kweon Kim(Seoul Nat' l Univ)

Abstract

A planar vibratory gyroscope using electrostatic actuation and electromagnetic detection is proposed. The gyroscope has large sensitivity and can be fabricated by using surface micromachining, bulk micromachining and conventional machining technology. In this paper, the gyroscope and the electromagnetic detecting system equations are derived to determine the output characteristics for the planar vibratory gyroscope using electrostatic actuation and electromagnetic detection. The maximum output is obtained when the driving frequency equals to the detecting frequency. The resonant frequencies of the resonator are determined by the beam stiffness, i.e. the material constants and spring dimensions. The dimensions of the beams are determined using the analytic vibration modelling. The expected resonant frequencies are 200Hz both and the sensitivity is 62mV/deg/sec with 4000 electronic circuit amplifying coefficient for an AC drive voltage of 3V with a DC bias voltage of 15V and DC field current of 50 mA.

Key Words: vibratory gyroscope (진동 자이로스코프), comb actuator(머리 빗 액츄에이터), electromagnetic detection(전자력 검출), polysilicon(폴리실리콘), resonant frequency (공진주파수)

1. Introduction

Future space applications require microspacecrafts that are lower in cost, mass, volume, and power consumption than present generation of spacecraft[1,2]. Micromachining technologies have become popular for fabricating small size gyroscopes. Recently, there have been many studies on planar vibratory gyroscopes[3-5], which rely on not the conservation of angular momentum of a rotating structure but the conservation of linear momentum of a vibrating structure. Most planar vibratory gyroscopes have been fabricated by a micromachining technology. Micromachined structures can withstand harsh environments for long periods of time, implying a lifetime not limited by the sensor element itself. They also have the additional advantages of small size, low price and low electric power consumption.

In this paper, a planar vibratory gyroscope using electrostatic actuation and electromagnetic detection is proposed to obtain a high sensitivity and a simple fabrication. The gyroscope is designed using a micromachining technology and a conventional macromachining technology. The gyroscope and the electromagnetic detecting system equations are derived to determine the output characteristics for planar vibratory gyroscope using electrostatic actuation and electromagnetic detection. The fabrication process of gyroscope is proposed using the (110) silicon bulk etching, surface micromachining and bonding technique. Finally, The feasibility of electromagnetic detection is demonstrated by the vibration test using the piezo actuator.

2. Structure and principle

The proposed gyroscope, as shown in Fig. 1, comprises a silicon resonator with polysilicon springs, sensing coils attached to the silicon resonator and field coils. The resonator is driven along X-direction by electrostatic force generated by AC voltage with DC bias voltage across the comb-actuators. The Coriolis force produced by an angular rate along Y-direction causes the resonator to oscillate in Z-direction. The oscillated displacement is detected using an induced voltage of the sensing coil which is generated by Faraday's law. The induced voltage is proportional to the angular rate.

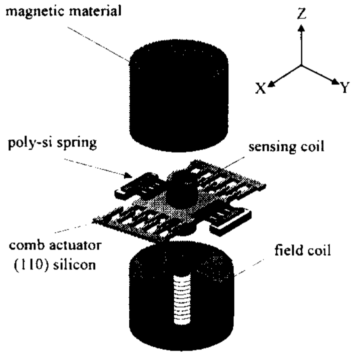

Fig. 1. The proposed planar vibratory gyroscope

3. Design of gyroscope

3.1 Electrostatic comb drive

Fig. 2 shows the linear resonator which can be driven differentially (push-pull) using the two combs. The derivative of the drive capacitance with respect to lateral displacement, $\partial C/\partial x$, is constant for the comb drive for displacements much less than the finger overlap.

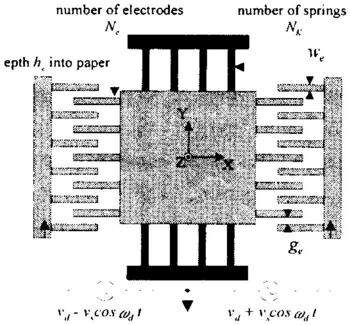

Fig. 2. Electrostatic comb drive

Therefore, the electrostatic force F_x^e is given by

$$F_x^e = 2\varepsilon_0 N_e \frac{h_e}{g_e} v_d v_s \cos\omega_d t \qquad (1)$$

where, h_e is height of electrode, g_e is gap of electrode, N_e is number of electrode, ω_d is exciting frequency, v_d is applied DC voltage and v_s is applied AC voltage

3.2 Resonant frequency

An accurate analytical expression for the resonant frequencies of the driving axis and the sensing axis can be found[6] as

$$f = \frac{1}{2\pi}\sqrt{\frac{2Ew_k(t_k/l_k)^3N_k}{M+0.375m}} \qquad (2)$$

where M and m are the masses of the silicon resonator and of the polysilicon spring and N_k is the number of springs. For fixed-fixed beam structure, an analytical expression K is given as

$$K_{sys} = \frac{2Ew_k t_k^3}{{l_k}^3} N_k \qquad (3)$$

where E is young's modulus, $I = (1/12)w_k t_k^3$ is the moment of inertia of the spring, and w_k, t_k, l_k are the width, the thickness and the length of the spring.

3.3 Motion equation

By the electrostatic force, the motion equation along X axis is

$$x(t) = \frac{F_0 Q_x}{K_x}\cos\omega_0 t \qquad (4)$$

where K_x is the stiffness of the polysilicon spring along X axis and Q_x is a quality factor. We assume the driving frequency of the resonator equals to the resonant frequency to obtain high sensitivity. The Coriolis force F_z^c produced by an angular rate Ω around the Y axis causes the resonator to oscillate in the Z axis.

$$z(t) = 2\Omega\frac{F_0 Q_x Q_z}{K\omega_0}\sin\omega_0 t \qquad (5)$$

where Ω is an angular rate, K_z is the stiffness of the polysilicon spring along Z axis and Q_z is quality factor. And we assume that the stiffness of polysilicon spring K_x and K_z equal to K to match the resonant frequencies along the X axis and Z axis.

3.4 Electromagnetic detecting system

As described above, applied angular rate leads to the vibration of the resonator and the sensing coil along Z axis. Fig. 3 shows the electromagnetic detecting system. When the coil vibrates along Z axis, the flux generated by the field coil varies sinusoidally. The flux density of air gap, generated by the field coil. Since the conductors pass through the magnetic field, an induced voltage V is generated in the sensing coil.

$$V = 2\pi r_m \frac{\mu_0 N_f N_s h_m}{g_m l_f} i v_z \qquad (6)$$

where N_f is the number of turns of field coil, i is applied current, g_m is the length of air gap, N_s is the number of turns of sensing coil, h_m is the thickness of the magnetic material, r_m is the mean radius of air gap, l_m is the height of the sensing coil and v_z is the velocity of the sensing coil.

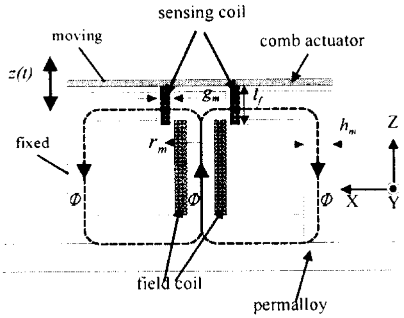

Fig. 3. Electromagnetic detecting system

3.5 Design of gyroscope

From above equations, we can derive the sensitivity of the gyroscope.

$$\frac{V}{\Omega} = 32\pi\mu_0\varepsilon_0 \, N_s N_f \frac{r_m h_m}{g_m l_s} N_e \frac{h_e}{g_e} \frac{1}{K} v_d v_s i Q_x Q_z \quad (7)$$

In this equation, the sensitivity depend on various parameters. Among these parameters, sensitivity is proportional to the height of the electrode and inversely proportional to the gap of electrode. The highest sensitivity for a vibratory gyroscope is obtained by thin and long spring and matching the resonant frequency of the two oscillatory modes(drive and detect). And the sensitivity to the angular rate is amplified by the Q factor of the resonance resulting in improved sensor performance.

Table 1 shows the design parameter of gyroscope.

Table 1. The design of gyroscope

<table>
<tr><td rowspan="2">comb electrode</td><td colspan="4">N_e</td><td colspan="4">h_e</td><td colspan="4">g_e</td></tr>
<tr><td colspan="4">233</td><td colspan="4">500㎛</td><td colspan="4">5㎛</td></tr>
<tr><td rowspan="2">polysilicon spring</td><td colspan="3">w_k</td><td colspan="3">t_k</td><td colspan="3">l_k</td><td colspan="3">K</td></tr>
<tr><td colspan="3">5㎛</td><td colspan="3">5㎛</td><td colspan="3">500㎛</td><td colspan="3">169</td></tr>
<tr><td rowspan="2">electromagnetic detecting system</td><td colspan="4">r_m</td><td colspan="4">h_m</td><td colspan="4">g_m</td></tr>
<tr><td colspan="4">2200㎛</td><td colspan="4">1500㎛</td><td colspan="4">850㎛</td></tr>
<tr><td rowspan="2">field coil & sensing coil</td><td colspan="4">l_f</td><td colspan="4">N_f</td><td colspan="4">N_s</td></tr>
<tr><td colspan="4">2000㎛</td><td colspan="4">1400</td><td colspan="4">377</td></tr>
<tr><td>resonant frequency</td><td colspan="6">f</td><td colspan="6">200Hz</td></tr>
<tr><td>sensitivity</td><td colspan="6">V/Ω</td><td colspan="6">62㎷/deg/sec</td></tr>
</table>

4. Test of electromagnetic detecting system

The verification of the electromagnetic detecting system was performed using the piezo actuator. Fig. 4 shows the experiment apparatus of the vibration test.

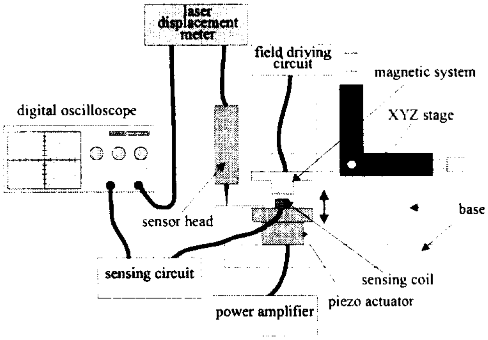

Fig. 4. Experiment apparatus

To vibrate the sensing coil, we used the piezo actuator. The displacement of piezo actuator measured by laser displacement meter(KEYENCE, LC-2420) and the output voltage are monitored simultaneously. The electromagnetic detecting system and sensing coil are assembled using XYZ stage.

Measurement were performed over a range of applied current from 20㎃ to 50㎃, displacements from 0.07㎛ to 0.21㎛. The frequency of the exciting voltage is 200Hz, which is the same with the expected resonant frequency. The detecting circuit consist of amplifiers, low-pass filter, and precision rectifier. Total amplifying gain is 2345, and the cut-off frequency is 1kHz.

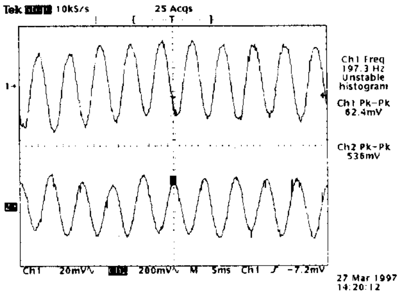

Fig. 5. Experimental Results (200Hz, 0.17㎛)

Fig. 5 shows the results of the vibration test. The upper waveform shows the displacement of sensing coil measured by the laser displacement meter, and lower waveform shows the output voltage measured in the sensing coil. Fig. 6 shows how the output voltage varies as we change the exciting current and the displacement of sensing coil. In this graph, solid lines indicate the results of the simulation, and the dots are the experimental data.

The output voltage is improved with an increase of the exciting current. When the exciting current increases, the linkage flux density increased. Also, since the induced voltage in the sensing coil is proportional to the velocity, the output voltage is improved with increased displacement of sensing coil.

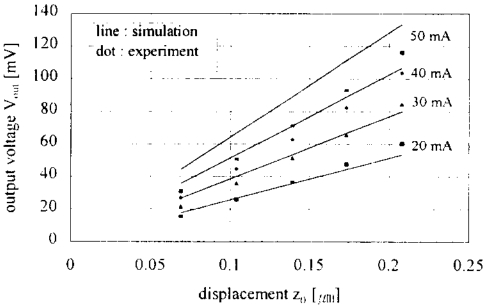

Fig. 6. Output voltage vs. displacement of the sensing coil

5. Fabrication process

The gyroscope structure are fabricated with the four-mask process.

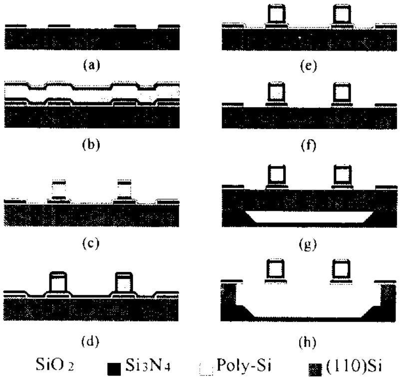

Fig. 7. Fabrication Process.

Fig. 7 shows the fabrication process of polysilicon spring structure. After alignment target etching, comb structure is patterned using the second mask. TEOS SiO_2 and LPCVD Si_3N_4 layer are deposited and patterned with the third mask, which defines the contact hole between polysilicon and (110) bulk silicon(Fig. 7.(a)). TEOS SiO_2 and LPCVD Si_3N_4 are deposited and 5μm thick polysilicon layer is then deposited by LPCVD. LPCVD Si_3N_4 and TEOS SiO_2 are deposited to pattern the polysilicon (Fig. 7.(b)). After patterning the polysilicon spring structure with the fourth mask (Fig. 7.(c)), LPCVD Si_3N_4 is deposited to passivate the polysilicon spring in silicon bulk etching(Fig. 7.(d)). Si_3N_4 is removed (Fig. 7.(e)) and SiO_2 passivation layer is removed (Fig. 7.(f)). (110) silicon and (100) silicon are bonded (Fig. 7.(g)). Finally, (110) silicon bulk etching is done (Fig. 7.(h)).

6. Conclusion

A planar vibratory gyroscope using electrostatic actuation and electromagnetic detection was proposed. Maximum output voltage is obtained when the resonant frequency of driving part equals to the resonant frequency of the sensing part. The expected sensitivities were varied by changing the exciting current and the velocity of the sensing parts. From the vibration test, the high sensitivity is obtained compared with electrostatic devices of which sensitivity is from several μV/deg/sec to several mV/deg/sec. Also, the sensitivity can be controlled easily by changing the number of turns of field and sensing coils, and the exciting current.

In conclusion, the proposed planar vibratory gyroscope using electrostatic actuation and electromagnetic detection, which has advantages of simple fabrication and large output characteristics, can be applied practically.

References

[1] T.K.Tang, R.C.Gutierrez, C.B.Stell and W.J.Kaiser, "A Packaged Silicon MEMS Vibratory Gyroscope for Microspacecraft," *MEMS Proceedings*, pp.500-505, 1997

[2] A.Lawrence, *Modern Inertial Technology : Navigation, Guidance, and Control*, Springer-Verlag, New York, 1993

[3] P.Greiff, B.Boxenhorn, T.King, and L. Niles, "Silicon Monolithic Micromechanical Gyroscope," *MEMS Proceeding* , pp. 966-968, 1991

[4] J.Bernstein, S.Cho, A.T.King, A.Kourepenis, P.Maciel,and M.Weinberg, "A micromachined Comb-Drive Tuning Fork Rate Gyroscope," *MEMS Proceeding*, pp.143-148, 1993

[5] K.Maenaka, T.Shiozawa, "A study of silicon angular rate sensors using anisotropic etching technology", *Sensors and Actuators* , A-43, pp. 72-77, 1994

[6] S.S.Rao, *Mechanical Vibrations*, Addison- Wesley, USA, 1990